Chinese Herbal Medicines 16 (2024) 151–161

Contents lists available at ScienceDirect

Chinese Herbal Medicines

journal homepage: www.elsevier.com/locate/chmed

Original Article

# Hypoglycemic activities of flowers of *Xanthoceras sorbifolia* and identification of anti-oxidant components by off-line UPLC-QTOF-MS/MS-free radical scavenging detection

Xiajing Xu [a], Yongli Guo [a], Menglin Chen [a], Ning Li [a], Yi Sun [b], Shumeng Ren [a], Jiao Xiao [a], Dongmei Wang [c], Xiaoqiu Liu [a,*], Yingni Pan [a,*]

[a] *School of Chinese Materia Medica, Key Laboratory for TCM Material Basis Study and Innovative Drug Development of Shenyang City, Shenyang Pharmaceutical University, Shenyang 110016, China*
[b] *Institute of Chinese Materia Medica, China Academy of Chinese Medical Sciences, Beijing 100700, China*
[c] *School of Pharmacy, Shenyang Pharmaceutical University, Shenyang 110016, China*

ARTICLE INFO

*Article history:*
Received 21 June 2022
Revised 27 July 2022
Accepted 11 November 2022
Available online 8 June 2023

*Keywords:*
anti-hyperglycemic activity
anti-oxidant
flowers of *Xanthoceras sorbifolia* Bunge
NADPH oxidase
off-line UPLC-QTOF-MS/MS-free radical scavenging

ABSTRACT

*Objective:* To identify phytochemical constituents present in the extract of flowers of *Xanthoceras sorbifolia* and evaluate their anti-oxidant and anti-hyperglycemic capacities.
*Methods:* The $AlCl_3$ colorimetric method and Prussian Blue assay were used to determine the contents of total flavonoids and total phenolic acids in extraction layers, and the bioactive layers was screened through anti − oxidative activity *in vitro*. The Waters ACQUITY UPLC system and a Waters ACQUITY UPLC BEH $C_{18}$ column (2.0 mm × 150 mm, 5 μm) were used to identify the ingredients. And anti-oxidative ingredients were screened by off-line UPLC-QTOF-MS/MS-free radical scavenging. The ameliorative role of it was further evaluated in a high-fat, streptozotocin-induced type 2 diabetic rat model and the study was carried out on NADPH oxidase (PDB ID: 2CDU) by molecular docking.
*Results:* Combined with the results of activity screening *in vitro*, the anti − oxidative part was identified as the ethyl acetate layer. A total of 24 chemical constituents were identified by liquid chromatography-mass spectrometry in the ethyl acetate layer and 13 main anti-oxidative active constituents were preliminarily screened out through off-line UPLC-QTOF-MS/MS-free radical scavenging. *In vivo* experiments showed that flowers of *X. sorbifolia* could significantly reduce the blood glucose level of diabetic mice and alleviate liver cell damage. Based on the results of docking analysis related to the identified phytocompounds and oxidase which involved in type 2 diabetes, quercetin 3-*O*-rutinoside, kaempferol-3-*O*-rhamnoside, isorhamnetin-3-*O*-glucoside, and isoquercitrin showed a better inhibitory profile.
*Conclusion:* The ethyl acetate layer was rich in flavonoids and phenolic acids and had significant anti-oxidant activity, which could prevent hyperglycemia. This observed activity profile suggested *X. sorbifolia* flowers as a promising new source of tea to develop alternative natural anti-diabetic products with a high safety margin.


## 1. Introduction

*Xanthoceras sorbifolia* Bunge (Wenguanguo in Chinese) is a Chinese tree species unique economic region, which is the family of Sapindaceae and widely cultivated in China. It has well-developed adaptability to extreme conditions against drought, cold, salt and starvation (N. Li et al., 2016; W. Li et al., 2020; Yao, Qi, & Yin, 2013). In addition, it plays important roles in the oil production for biodiesel, foods, fodders, medicines and industrial chemicals (Yao, Qi, & Yin, 2013; Wang, Jiang, Meng, & Li, 2011). However, the low fruit-setting rate, small percentage of fine breeds, high development cost, and low economic efficiency retarded the development of *X. sorbifolia* presently (Yao, Qi, & Yin, 2013; Bi, Cai, Ma, Yang, & Guan, 2011). Therefore, it is urgent to develop and utilize other parts of *X. sorbifolia*, so as to improve its resource utilization.

Tea is one of the most popular beverages all over the world and its quality and safety attract considerable research attention (Tounekti, Joubert, Hernandez, & Munne-Bosch, 2013). However, the plant is prone to attack by an array of pests and diseases

* Corresponding authors.
*E-mail addresses:* liuxiaoqiu3388@126.com (X. Liu), panyingni@163.com (Y. Pan).

https://doi.org/10.1016/j.chmed.2022.11.009
1674-6384/

throughout the year (Jiang et al., 2020). A concern for human health and environmental safety demands foods free of pesticide residues and tea is no exception to this. Hence, it has focused on screening out safe and pollution-free scented tea. Flower of *X. sorbifolia*, notoriously referred to as "thousands of flowers but one fruit" (Bi, Cai, Ma, Yang, & Guan, 2011), is harvested from April to May, when *X. sorbifolia* is not infected by pests and not sprayed with pesticides. Phytochemical studies have been performed that *X. sorbifolia* is a rich source of effective flavonoids, coumarins, steroids, terpenoids, organic acids, which have been proved to have many biological activities such as anti-oxidation, hypoglycemic activity, anti-inflammatory activity, etc. (Cao, Xia, Chen, Xiao & Wang, 2013; Godoy et al., 2013; Li et al., 2016; Zhao et al., 2018; Wu, Liu, Qin, Wang & Wu, 2019; Li et al., 2020; Wang et al., 2016). However, the previous research of *X. sorbifolia* was mostly focused on the husk, carpophore, testa, and few studies on flower. Owing to its potential in nutrition and health, the use of *X. sorbifolia* flowers as a tea is of paramount importance to improve the resource utilization of it.

In recent years, ultra high performance liquid chromatography-mass spectrometry technology coupled with chemical reaction has been developed to quickly identify active components in the natural plants. Free radicals are products of normal metabolism of human body and also important components of immune system, but excess free radicals can cause various chronic diseases such as cancer, cardiovascular diseases, as well as various diseases associated with aging. Therefore, eliminating excess free radicals in the body plays an important role in the treatment of diseases and everyday life. The ultra high performance liquid chromatography (UPLC) was coupled with free radicals to compare the change rate of peak area between samples and free radicals before and after the UPLC reaction, which directly reflected the anti-oxidant active components in natural plants (Zhao, Wang, Jiang, & Li, 2017; Yang, Li, & Li, 2018). Therefore, off-line UPLC-QTOF-MS/MS coupled with free radical was used to identify anti-oxidant components in flowers of *X. sorbifolia*, which provided a method for rapidly screening of bioactive substances.

Diabetes mellitus is a group of systemic metabolic disorders with a high rate of morbidity and mortality worldwide (Jessica et al., 2017). Many factors (internal and external), such as obesity, sedentary lifestyle, and oxidative stress, are directly involved in these cell alterations (Etsassala et al., 2020). Normal cellular homeostasis is maintained by the balance between endogenous pro-oxidant enzymes (NADPH oxidase), oxidants and endogenous anti-oxidants (Mazumdar, Marar, Devarajan, & Patki, 2021). Growing evidences suggested that hyperglycemia can disturb the anti-oxidant-prooxidant balance through activation of NADPH oxidase to increase the level of intracellular reactive oxygen species (ROS) (Najafi, Kavoosi, Siahbalaei, & Kariminia, 2022). Excessive ROS leads to the disruption of redox signaling and to molecular damage, which can result in cell death and various metabolic disorders would ultimately possibly be induced (Najafi, Kavoosi, Siahbalaei, & Kariminia, 2022). Regrettably, there is currently no cure available for diabetes, but it can be managed by controlling blood sugar levels through a healthy diet, exercise, and medication, which can reduce the risk of long-term diabetes complications (Etsassala et al., 2020). Therefore, there is a great need in developing alternative natural anti-diabetic products with a high safety margin.

The present study aimed to identify phytochemical constituents present in the extract of flowers of *X. sorbifolia* and evaluate their anti-oxidant and anti-hyperglycemic capacities. According to the qualitative phytochemical results by UPLC-QTOF-MS/MS, anti-oxidant compounds were screened by off-line UPLC-QTOF-MS/MS-free radical scavenging detection. Additionally, the ameliorative role of it in a high-fat, streptozotocin-induced type 2 diabetic rat model was evaluated, whereas a docking analysis was conducted to confirm the interactions between selected phytochemicals and enzymes. It is expected that data generated from this investigation will provide valuable insights on the pharmacological potential of *X. sorbifolia* flowers, thus developing the new uses of this plant.

## 2. Materials and methods

### 2.1. Plant material and preparation of extracts

Flowers of *X. sorbifolia* were collected from Chifeng, Inner Mongolia, China in 2020 which were identified by chief pharmacist Weining Wang, Liaoning Provincial Institute for Drug Inspection and Testing. ABTS was purchased from Sigma Aldrich (30931–67-0, St. Louis, MO, USA). Potassium persulfate (KPS) was prepared from Amresco (216224, Solon, OH, USA); DPPH was from Macklin Biochemical Co., Ltd. (19898–66-4, Shanghai, China). Vitamin C (Vc) (purity > 98%) was obtained from Tianjin Yongda Chemical Reagengt Co., Ltd. (20211216, Tianjin, China). Chromatographic grade methanol was purchased from Sigma Aldrich. Other reagents were analytical grade.

Dried flowers of *X. sorbifolia* (5 g) were extracted three times with water for 3 h. The extract of it was suspended in distilled water and partitioned with ethyl acetate (EtOAc), and *n*-butanol (*n*-BuOH) to EtOAc, *n*-BuOH, and water fractions.

### 2.2. Profile of bioactive compounds and determination of anti-oxidant effects

Dried flowers of *X. sorbifolia* were extracted with 10 mL of water for 1.5 h. The flowers solution was stored at − 20 °C. The content of total flavonoid (TFC) was estimated by $AlCl_3$ colorimetric method (Zhang, Luo, Huan, Cai, & Zhang, 2018). The content of total phenol (TPC) was determined by a modified the Prussian Blue assay (Gao, Chen, He, Sun & Zeng, 2018).

DPPH scavenging activity, with $V_C$ as standard, was assayed as previously reported procedures (Ma, Feng, Diao, Zeng, & Zuo, 2020). The scavenging activity of $ABTS^+$ free radical was determined by a modified method (Guo et al., 2020). The scavenging activity of OH was measured according to the modified procedure (Wang, Pu, Jiang, & Fu, 2017). The activity of FRAP was determined by the improved method (Qi et al., 2019).

### 2.3. UPLC-ESI-QTOF-MS analysis

Chromatographic separation was performed on Acquity UPLC system (Waters, Massachusetts, USA). An Acquity UPLC BEH $C_{18}$ column (2.0 mm × 150 mm, 5 μm, Waters, Massachusetts, USA) was used at temperature of 35 °C. The mobile phases consisted of eluent A (0.1% formic acid-acetonitrile, volume percent) and B (0.1% aqueous formic acid, volume percent) at flow rate of 0.4 mL/min with a liner gradient program: 0–8 min, A from 20%−29%; 8–13 min, A from 29%−39%. Data acquisition and processing were performed using MassLynx software.

The Acquity UPLC system was coupled to Waters Xevo G2 QTOF (Waters, Milford, MA, USA). Mass Spectrometer was equipped with electrospray ionization (ESI). The instrument was operated in negative ion mode to perform full scan monitoring on the range of *m*/*z* 100–1 200. The other operating parameters were set as follow: capillary voltage of 1.0 kV; sample cone voltage of 40 V; source temperature of 120 °C, desolvation temperature 500 °C and desolvation gas flow of 800 L/h. In MSE mode, trap collision energy of low energy function was set at 6 eV, while ramp trap collision energy of high energy function was set at 20–60 eV.

### 2.4. Off-line UPLC-QTOF-MS/MS-free radical scavenging detection

#### 2.4.1. DPPH-UPLC analysis

Extract/fraction (1 mL, 0.2 mg/mL in methanol) was reacted with DPPH• (1 mL, 0.2 mg/mL in methanol) at 37 °C for 30 min. Then the mixtures were passed through a 0.22 μm filter before UPLC analysis. Sample (mg/mL) without the addition of DPPH• was used as a control. The area integral and relative standard deviation of the chromatographic peak of the sample were calculated. The percentage of peak area decrease was calculated according to the formula. The reaction ability of the sample with DPPH free radical was expressed as Equation (1):

$$RP(\%) = (A_0 - A_1)/A_0 \times 100 \quad (1)$$

where $RP$ is the reduction of the peak area, $A_0$ is the peak area of the sample, $A_1$ represents the sample peak area after reaction with free radical.

#### 2.4.2. ABTS-UPLC analysis

Extract/fraction (1 mL, 1 mg/mL) was reacted with ABTS• (1 mL, Abs = 700 nm in methanol) at 37 °C for 30 min. Then the mixtures were passed through a 0.22 μm filter before UPLC analysis. Sample (mg/mL) without the addition of ABTS• was used as a control. The reaction ability of the sample with ABTS free radical was expressed as Equation (1).

#### 2.4.3. OH-UPLC analysis

The mixture which was consisted of 0.5 mL of ferrous sulfate (9 mmol/L), 0.5 mL of hydrogen peroxide (8.8 mmol/L), 0.5 mL of the samples was incubated at 25 °C for 10 min. The 0.5 mL of sodium salicylate (9 mmol/L) was incubated at 37 °C for 30 min. The mixtures were then passed through a 0.22 μm filter before UPLC analysis. Sample (1 mg/mL) without the addition of hydrogen peroxide was used as a control. The reaction ability of the sample with OH• free radical was expressed as Equation (1).

### 2.5. Hypoglycemic effect of EtOAc layer on streptozotocin (STZ)-induced diabetic mice

#### 2.5.1. Animal experiments

Six-week-old male C57BL/6 mice (weight 18–22 g) were purchased from Liaoning Changsheng biotechnology Co., Ltd., China (SYXK (Liao) 2020–005) and were bred adaptively for 7 d in standard conditions with a temperature (25–28 °C), humidity (50%–60%) and a 12-h light–dark cycle and food and water were freely obtained. All animal procedures were performed by the NIH guidelines and approved by the Ethical Committee of Shenyang Pharmaceutical University (SYPU-IACUC-C2019-7–06-204).

After one week of adaptive feeding, five mice were randomly assigned to the control group and fed normally, while the other mice were assigned to the experimental group and fed with high-sugar and high-fat feed (basic food 59.5%, sucrose 20%, lard oil 10%, yolk powder 10% and sodium cholate 0.5%). After two weeks of feeding, mice in the experimental group were injected intraperitoneally for five consecutive days with 50 mg/kg streptozocin (Sigma-Aldrich, Shanghai, China) to induce diabetes (Li et al., 2020), and mice in control group received vehicle buffer alone. After 3 d fasting blood glucose (FBG) higher than 11.1 mmol/L was considered as the basis for the success of the diabetic model. The high-sugar and high-fat diet was continued in diabetic mice throughout the course of the study. Diabetic mice were divided into five groups. There were one model group and four therapy groups including the low, medium, high *X. sorbifolia* groups [received 30, 60 and 90 mg/(kg·d) EtOAc effect of *X. sorbifolia*, respectively] and metformin group [200 mg/(kg·d)], orally by daily gavage for a period of 15 d. Fasting blood glucose level of mice was tested every five days.

Oral glucose tolerance test (OGTT) was performed in 12 h fasted mice on 14th day of the treatment. The mice were fasting overnight before the administration of an oral glucose load [2.5 mg/(kg·d) of body weight]. Blood samples were collected from the tail vein at 0, 30, 60, 90, and 120 min after the glucose administration. All data referring to blood glucose levels were achieved by a blood glucose meter (Sinocare Inc., Changsha, China). All mice were euthanized to collect blood samples at the end of experiments.

#### 2.5.2. Biochemical analysis

Serum biochemical parameters including total cholesterol (TC), triglycerides (TG), low-density lipoprotein cholesterol (LDL-C), and high-density lipoprotein cholesterol (HDL-C) were detected by relevant assay kit (JianchengBio, Nanjing, China).

#### 2.5.3. Histopathology analysis

Liver tissue for histopathological analysis was preserved in 10% buffered formalin saline, and then embedded in paraffin. Tissue wax was sliced into 4 mm sections. Fixed sections were then stained with haematoxylin-eosin (H&E). Stained slides were analyzed under an optical microscope.

#### 2.5.4. Molecular docking

The structures of 13 compounds which were screened by off-line UPLC-QTOF-MS/MS-free radical scavenging were sketched in the Chemdraw Ultra 6.0 module of Chem. Office 6.0. The sketched molecules were copied and pasted to Chem 3D saved in a mol format, followed by the energy minimization of the structure. The three-dimensional structure of NADPH oxidase (PDB ID: 2CDU) was retrieved from the RCSB PDB (https://www.rcsb.org/pdb/home/home.do). The molecular docking analysis of the main compounds to oxidase was performed by the Surflex-Dock Geom (SFXC) mode using SYBYL-X 2.0 software package (Tripos, Inc., St. Louis, MO, USA). Subsequently, a docking score file was generated and saved as the SD format. A C-Score (≥4) was selected as the credible results for the next docking analysis. The Surflex-Dock scoring function is a weighted sum of non-linear functions involving van der Waals surface distances between the appropriate pairs of exposed enzyme and ligand atoms.

### 2.6. Statistical analysis

All values were exhibited as means ± SD. One-way analysis of variance (ANOVA) and student's *t*-test were used. Results were considered statistically significant when $P < 0.05$.

## 3. Results and discussion

### 3.1. Phytochemical profile and anti-oxidant activities

The standard assessment of bioactive compounds, in terms of phenolic and flavonoid contents was presented in Fig. 1. Phenols and flavonoids were highly enriched in EtOAc layer with values of (66.88 ± 0.19) GAE/g, (12.55 ± 0.42) mg RE/g, which were 2.7 and 4 times higher than those detected in crude extracts and 8.7 and 18.5 times higher than those detected in water layer. The results indicated that the TPC and TFC were higher in EtOAc layer, and it was an excellent solvent for the enrichment of phenols and flavonoids.

Assessing anti-oxidant properties of plant extracts is crucial in the evaluation of plants' bioactivity and plants' ability to prevent and/or mitigate health problems. Investigations have demonstrated that intake of anti-oxidants could prevent or delay the

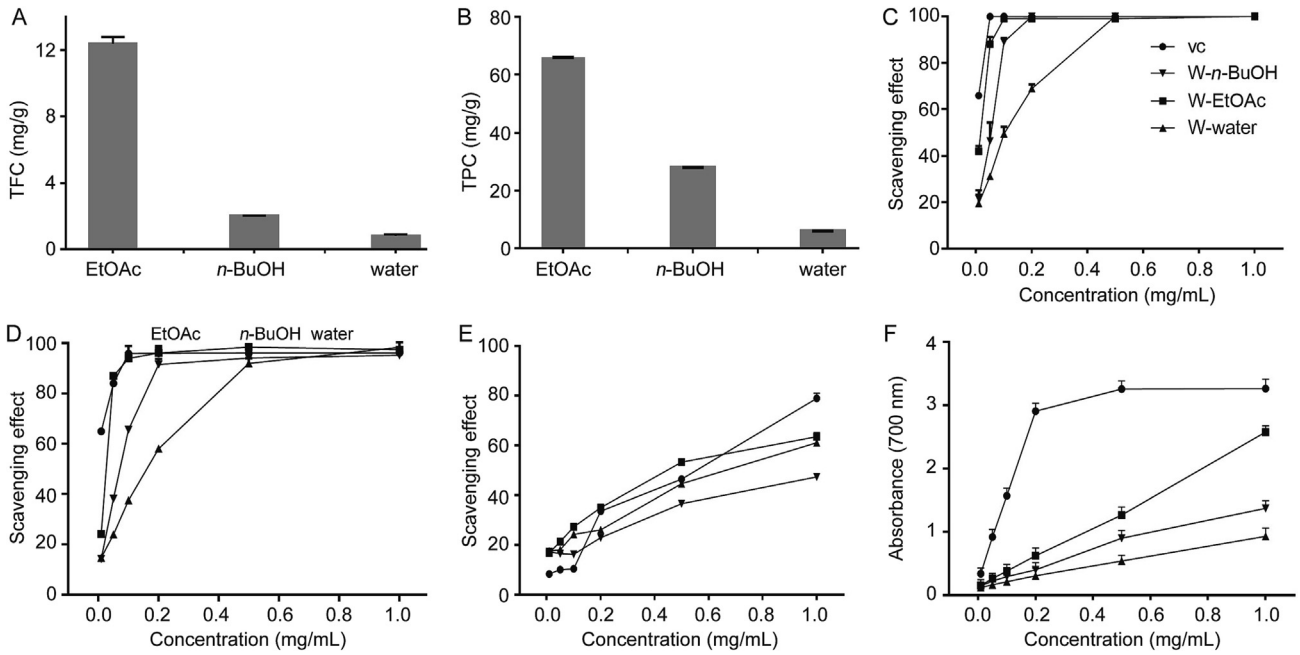


**Fig. 1.** TFC (A) and TPC (B) contents of flowers of *X. sorbifolia* fraction. Anti-oxidant activity of crude extract and sub-fractions of flowers of *X. sorbifolia*; C: DPPH radical scavenging activities; D: ABTS radical scavenging activities; E: OH radical scavenging activities; F: reducing power.

onset/progress of several human ailments (Wu, Liu, Qin, Wang, & Wu, 2019). In order to obtain a comprehensive understanding of the anti-oxidant potential of *X. sorbifolia* flowers, multiple anti-oxidant assays were employed. At concentrations of 0.5 mg/mL, the EtOAc and *n*-BuOH showed the DPPH radical and ABTS free radical inhibition rates were above 90%. As can be seen from Fig. 1E and F, the scavenging ability of each fraction of flowers of *X. sorbifolia* to OH free radical and the ferric reducing power were weaker than that of DPPH and ABTS free radical. EtOAc layer had the strongest ability of scavenging OH radical and exhibited the strongest reducing power. In addition, $IC_{50}$ values of the scavenging ability of the three compounds on four free radicals were calculated (Table. 1). It was found that the EtOAc layer had a good scavenging ability of DPPH radical and ABTS free radical inhibition rates.

### 3.2. Identification of ethyl acetate fraction by UPLC-ESI-QTOF-MS

In this study, the elution situation of methanol–water and acetonitrile–water mobile phase system were compared, and the acetonitrile–water mobile phase system was obviously superior. Taking acetonitrile–water as mobile phase, the mobile phase acetonitrile–water (80:20, 50:50, 20:80) and gradient elution were compared, and gradient elution was better. The peak shape was improved by adding formic acid, so the gradient elution acetonitrile–water-formic acid was adopted.

The TOF-MS technique was a high-resolution, large mass range and high-sensitivity method that was especially suitable for the accurate molecular weight determination of total flavonoids and phenol contents (Wu et al., 2016). Because of the high contents of total phenolic acids and total flavonoids and good anti-oxidant activity of ethyl acetate fraction, the compounds were identified by UPLC-ESI-QTOF-MS. A total of 24 compounds were identified according to their retention times, the deprotonated macular ions ($[M-H]^-$, negative ion mode) and the characteristic product ions in comparison with those of authentic standards and literature data. The main aglycones of 24 compounds were myricetin, kaempferol, quercetin, isorhamnetin, chrysoeriol (Fig. 2). The data of retention time, maximum absorbance, molecular ions $[M-H]^-$, and the characteristic product ions were summarized in Table 2.

#### 3.2.1. Identification of quercetin derivatives

In this study, seven quercetins and their derivatives were detected in EtOAc layer. Peak 21 ($t_R$ 10.35 min, *m*/*z* 302) was identified as quercetin (Hui et al., 2017), with $[M-H]^-$ at *m*/*z* 301 and fragments at *m*/*z* 301, 300, 271, 255, 243. The major product ions and their intensity of peak 16 were similar to peak 21, but they had different retention time which was due to their different substituted hexoside. We supposed the hexoside of peak 2 to be glucoside, namely peak 16 was isoquercitrin. The conclusion was further confirmed by comparing the mass spectrum and chromatography with an authentic standard (Hui et al., 2017; Braunberger et al., 2013). It was obvious that compounds **1**, **6**, **11**, **12** and **13** showed the same fragment ions at *m*/*z* 301, which was decided to be the quercetin mother ring. The fragment ions *m*/*z* 301 $[M-H-308]^-$ at the 11th and 12th peaks represented the structure of the quercetin unit, the glycosyl residue (*m*/*z* 308) and one hexose units, and one deoxyhexose unit were observed.

Based on the low abundances of its deprotonated aglycone from peak 11, the neutral loss of 308 amu might be related to the glyco-

**Table 1**
Anti-oxidant activities of flowers of *X. sorbifolia*.

| Samples | $IC_{50}$ in DPPH• (mg/mL) | $IC_{50}$ in •OH (mg/mL) | $IC_{50}$ in $ABTS^{+}$• (mg/mL) | Reducing power |
|---|---|---|---|---|
| Dried flowers | 0.279 ± 0.008 | 2.724 ± 0.335 | 0.16 ± 0.010 | 0.880 ± 0.010 |
| W-EtOAc | 0.019 ± 0.000 | 0.463 ± 0.048 | 0.012 ± 0.001 | 2.578 ± 0.100 |
| W-*n*-BuOH | 0.055 ± 0.001 | 2.531 ± 0.076 | 0.027 ± 0.001 | 1.375 ± 0.121 |
| W-water | 0.112 ± 0.006 | 0.777 ± 0.007 | 0.073 ± 0.004 | 0.93 ± 0.133 |

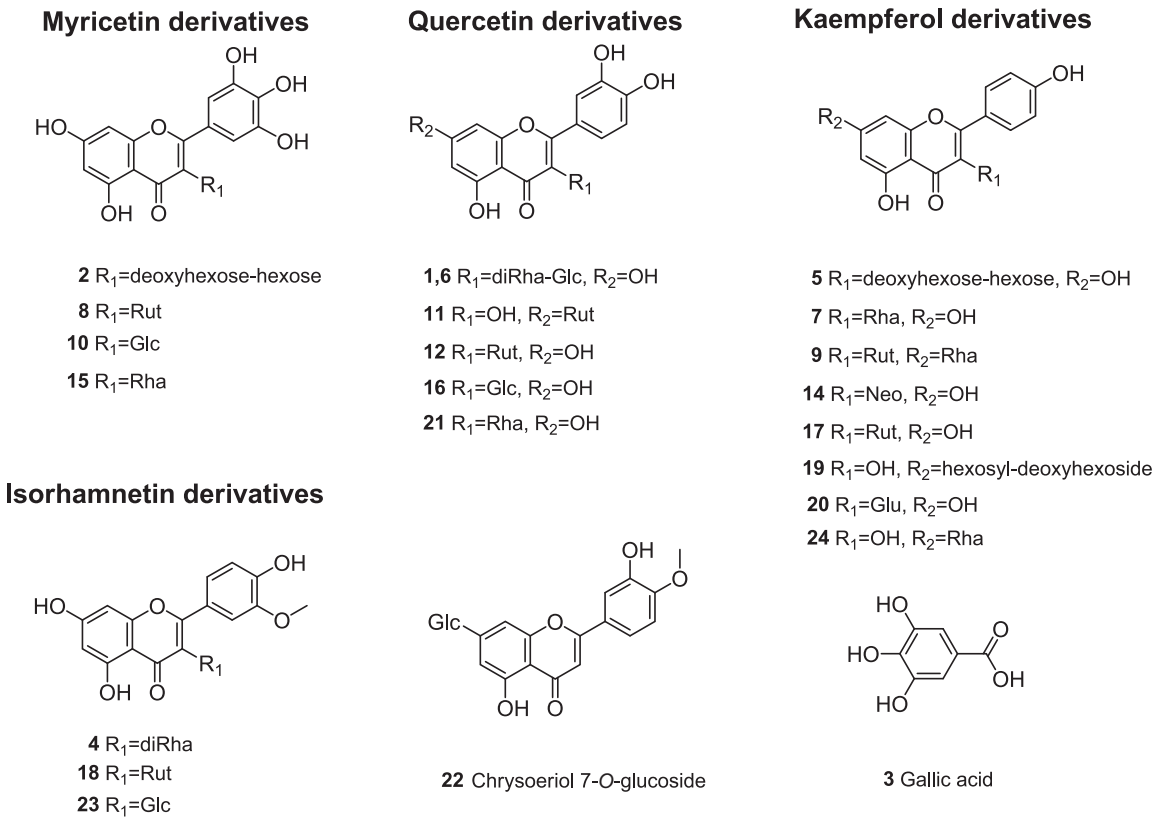


**Fig. 2.** Structural skeletons of flavonoids and phenolic acids in EtOAc layer.

sylic fragmentation in position 5. Thus, it was deduced that this compound was quercetin-7-*O*-rutinoside. Additionally, the abundance of fragment ions $[Y0\text{-}H]^{-}\bullet$ at *m*/*z* 300 were higher than that of $Y0^{-}$ at *m*/*z* 301, indicating the glycosylation positions of quercetin at 3-OH. It was deduced that peak 12 was quercetin 3-*O*-rutinoside. The compounds corresponding to peaks 1 and 6 had the same fragment ion at *m*/*z* 755 $[M-H]^{-}$. The major fragments from peak 8, at *m*/*z* 593 [(M−H)-162]$^{-}$, *m*/*z* 301 $Y0^{-}$, *m*/*z* 300 $[Y0\text{-}H]^{-}$ indicated it to quercetin 3-*O*-dirhamnosyl-glucoside. In addition, the missing of 146u and 162 from $[M-H]^{-}$ of the compound suggested the sugars attached to the quercetin aglycon were deoxyhexose and hexose. Peak 13 was tentatively characterized as quercetin-7-*O*-dirhamnosyl-diglucoside.

### 3.2.2. Identification of kaempferol derivatives

Peaks 20 and 7 were characterized as kaempferol 3-*O*-Glucoside ($[M-H]^{-}$ at *m*/*z* 447) and kaempferol 7-*O*-rhamnoside ($[M-H]^{-}$ at *m*/*z* 431). The abundance of fragment ions $[Y0\text{-}H]^{-}\bullet$ at *m*/*z* 284 were higher than that of $Y0^{-}$ at *m*/*z* 285, indicating the glycosylation positions of quercetin at 3-OH. In addition, the missing of 162u and 146u from $[M-H]^{-}$ of the compound suggested that the sugars attached to the kaempferol aglycon were hexose and deoxyhexose. Compounds 5, 7, 9, 14, 17, and 24 had identical fragment ions at 285, 284, and 255, as well as 227, suggesting that they were derivatives of kaempferol. Peak 5 had the fragment ion at *m*/*z* 593 $[M-H]^{-}$. However, the main fragments of *m*/*z* 285 $Y0^{-}$ [(M−H)-146–308] and *m*/*z* 284 $[Y0\text{-}H]^{-}$ showed that the compound was sahniphenol-3-deoxyhexose hexose. Peaks 14 and 17 were determined as kaempferol-3-*O*-neohesperidoside ($[M-H]^{-}$ at *m*/*z* 593), kaempferol 3-*O*-rutinoside ($[M-H]^{-}$ at *m*/*z* 593), respectively. The relative abundance of the fragment ion $[Y0\text{-}H]^{-}$ at peak 17 *m*/*z* 284 was higher than that of the fragment ion Y0 at peak 17 *m*/*z* 285, indicating that the two compounds were kaempferol 3-*O*-neohemperidin and kaempferol 3-*O*-rutin. Peak 24 was assigned as kaempferol-7-*O*-rhamnoside, based on the existence of the fragment ions $Y0^{-}$ at *m*/*z* 285 (missing of deoxyhexose), indicating the glycosylation positions of kaempferol at 7-OH. Peak 9 had the fragment ion at *m*/*z* 739 $[M-H]^{-}$, but the major fragments at *m*/*z* 593 [(M−H)-146]$^{-}$, *m*/*z* 285 $Y0^{-}$ [(M−H)-146–308]$^{-}$, *m*/*z* 284 $[Y0\text{-}H]^{-}$ revealed that the compound was kaempferol 3-*O*-rutinoside7-*O*-rhamnosyl (Fig. 3).

### 3.2.3. Identification of isorhamnetin derivatives

Peak 23 was characterized as isorhamnetin-7-*O*-glucoside ($[M-H]^{-}$ at *m*/*z* 477), on the basis of the existence of the fragment ions $[Y0\text{-}H]^{-}\bullet$ at *m*/*z* 315, which correspond to kaempferol aglycones, *m*/*z* 300 (losses of $CH_3$ from *m*/*z* 315), *m*/*z* 271 (losses of $CH_3$ and CO from *m*/*z* 315) corresponding to the characteristic fragment ions of aglycone. In addition, the missing of 162u from $[M-H]^{-}$ of the compound suggested the sugars attached to the isorhamnetin aglycon were hexose. It was obvious that compounds **4** and **18** had the same fragment ions at 315, 300, 271 with 23, indicating that they were isorhamnetin derivatives. The compounds corresponding to peaks 4 and 18 had the fragment ion at *m*/*z* 609 $[M-H]^{-}$ and *m*/*z* 623 $[M-H]^{-}$, but the major fragments at *m*/*z* 462 [(M−H)-146]$^{-}$, *m*/*z* 315 $[Y0\text{-}H]^{-}$ for peak 4 revealed the compound to be isorhamnetin 3-*O*-dirhamnosyl. The major fragment at peak 18 *m*/*z* 315 $[Y0\text{-}H]^{-}$ $(M-H)^{-}308$ showed isorhamnetin 3-*O*-rutin.

### 3.2.4. Identification of myricetin derivatives

On the basis of the existence of the fragment ions $[Y0\text{-}H]^{-}\bullet$ (*m*/*z* 316), the 15th and 10th peaks were respectively characterized as myricetin ($[M-H]^{-}$ at *m*/*z* 463) and myricetin 3-*O*-glycoside ($[M-H]^{-}$ at *m*/*z* 479). In addition, the missing of 162u and 146u from $[M-H]^{-}$ in the compound suggested the sugars attached to the myricetin aglycon were hexose and deoxyhexose. Compounds **2**, **10** and **15** had the same fragment ions at *m*/*z* 287 and 271, indi-

**Table 2**
Analyses of flavonoids and phenolic acids in EtOAc layer by UPLC-ESI-QTOF-MS.

| Peak No. | $t_R$ (min) | Molecular formula | Experiment | MS/MS fragmentation | Identification | References |
|---|---|---|---|---|---|---|
| 1 | 4.06 | $C_{33}H_{40}O_{20}$ | 755.132 2 | 609, 463, 301, 300, 271, 255 | Quercetin 3-*O*-glucoside-dirhamnosyl | |
| 2 | 4.3 | $C_{27}H_{30}O_{17}$ | 625.078 6 | 316, 271 | Myricetin 3-*O*-neohesperidoside | |
| 3 | 4.84 | $C_7H_6O_5$ | 168.988 1 | 126 | Gallic acid | (Vieira, Marques, Machado, Sliva, & Hubinger, 2017) |
| 4 | 5.33 | $C_{28}H_{32}O_{15}$ | 609.084 0 | 462, 315, 300, 284, 271 | Isorhamnetin-3-*O*-dirhamnosyl | |
| 5 | 5.48 | $C_{27}H_{30}O_{15}$ | 593.089 4 | 284, 255, 227 | Kaempferol-3-*O*-deoxyhexose-hexose | |
| 6 | 5.77 | $C_{27}H_{30}O_{15}$ | 755.132 2 | 593, 300, 271, 255 | Quercetin-3-*O*-dirhamnosyl-glucoside | (Tkacz et al., 2020) |
| 7 | 5.95 | $C_{21}H_{20}O_{10}$ | 431.143 6 | 284, 255, 285, 271, 227 | Kaempferol-3-*O*-rhamnoside | (Khallouki, Ricarte, Breuer, & Owen, 2018) |
| 8 | 6.22 | $C_{27}H_{30}O_{17}$ | 625.078 6 | 316, 287, 271 | Myricetin-3-*O*-rutinoside | (Wu et al., 2016) |
| 9 | 6.62 | $C_{33}H_{40}O_{19}$ | 739.137 6 | 593, 284, 255, 151 | Kaempferol-3-*O*-rutinoside-7-*O*-rhamnoside | |
| 10 | 6.83 | $C_{21}H_{20}O_{13}$ | 478.874 4 | 316, 317, 287, 271, 243 | Myricetin 3-*O*-glucoside | (Zheng et al., 2019) |
| 11 | 6.94 | $C_{27}H_{30}O_{16}$ | 609.084 | 301, 300, 271, 255, 227 | Quercetin 7-*O*-rutinoside | (Cao, Xia, Chen, Xiao, &Wang, 2013) |
| 12 | 7.48 | $C_{27}H_{30}O_{16}$ | 609.078 | 301, 300, 271, 255 | Quercetin 3-*O*-rutinoside | (Zheng et al., 2019) |
| 13 | 7.84 | $C_{42}H_{46}O_{22}$ | 900.940 4 | 755, 609, 447, 301, 300 | Quercetin-7-*O*-dirhamnosyl-diglucoside | |
| 14 | 8.05 | $C_{27}H_{30}O_{15}$ | 593.092 6 | 284, 285, 255, 227 | Kaempferol 3-*O*-neohesperidoside | (Wang et al., 2014) |
| 15 | 8.22 | $C_{21}H_{20}O_{12}$ | 463.037 8 | 317, 316, 271, 259 | Myricitrin | (Unuofin & Lebelo, 2021) |
| 16 | 8.48 | $C_{21}H_{20}O_{12}$ | 463.0378 | 301, 300, 271, 255, 243, 227 | Isoquercitrin | (Braunberger et al., 2013) |
| 17 | 8.93 | $C_{27}H_{30}O_{15}$ | 593.092 6 | 285, 255, 227 | Kaempferol-3-*O*-rutinoside | Vieira, Marques, Machado, Silva, & Hubinger, 2017 |
| 18 | 9.26 | $C_{28}H_{32}O_{16}$ | 623.098 | 463, 315, 300, 271, 255 | Isorhamnetin 3-*O*-rutinoside | Tkacz et al., 2020 |
| 19 | 9.63 | $C_{26}H_{28}O_{16}$ | 554.203 1 | 300, 284, 271, 255, 227 | Kaempferol-7-*O*-hexosyl(1–2) deoxyhexoside | |
| 20 | 10.06 | $C_{21}H_{20}O_{11}$ | 447.043 7 | 284, 255, 227 | Kaempferol 3-*O*-glucoside | Vieira, Marques, Machado, Silva, & Hubinger, 2017 |
| 21 | 10.35 | $C_{21}H_{20}O_{11}$ | 447.043 7 | 301, 300, 271, 255, 243, 227 | Quercitrin | Hui et al., 2017 |
| 22 | 11.60 | $C_{22}H_{22}O_{11}$ | 460.903 0 | 299, 297, 284, 269, 255 | Chrysoeriol 7-*O*-glucoside | Zheng et al., 2019 |
| 23 | 12.17 | $C_{22}H_{22}O_{12}$ | 476.894 5 | 390, 315, 300, 272, 255 | Isorhamnetin-3-*O*-glucoside | Khallouki, Ricarte, Breuer, & Owen, 2018 |
| 24 | 12.45 | $C_{21}H_{20}O_{10}$ | 430.901 3 | 285, 255, 227 | Kaempferol 7-*O*-rhamnoside | Hui et al., 2017 |

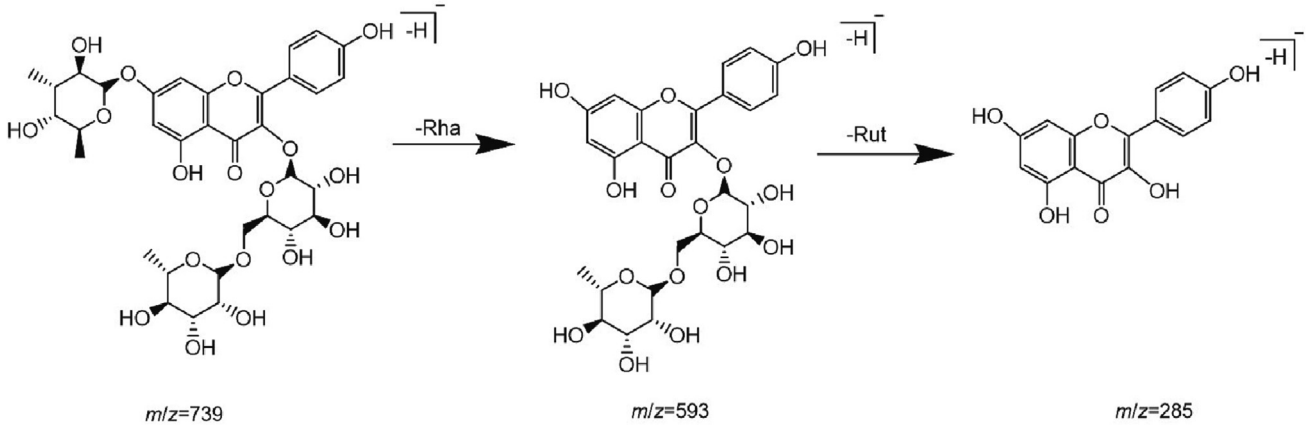


**Fig. 3.** Mass spectrum and fragmentation pathway of flavonoid *O*-glycosides (Compound 9 was explained in detail as examples here).

cating that they were myricetin derivatives. On the basis of the relative abundance of the fragment ion Y0$^-$ at *m*/*z* 317, peaks 2 and 8 were determined as myricetin-3-*O*-neohesperidoside ([M−H]$^-$ at *m*/*z* 625), myricetin 3-*O*-rutinoside ([M−H]$^-$ at *m*/*z* 625), respectively.

### 3.2.5. Identification of other compounds

Peak 3 was compared with the mass spectral data reported by Marzouk (2008), and was shown to be gallic acid, on the basis of the existence of the fragment ions 168.8941 [M−H]$^-$ and 126 [M−H−COO]$^-$. Peak 22 was characterized as chrysoeriol-7-*O*-glucosid ([M−H]$^-$ at *m*/*z* 461).

### 3.3. Off-line UPLC-QTOF-MS/MS-free radical scavenging detection

LC-free radical was used as a rapid method to screen anti-oxidants from complex mixtures. It was believed the structure of anti-oxidants will be changed after they reacted with free radical. The identities of the “hits” were further identified by off-line UPLC-QTOF-MS/MS-free radical scavenging detection analysis,

then the anti-oxidant activity of compounds could be evaluated by the change of peak area (Fig. 4). Table 3 displayed the differences of the peaks in the reduction of the peak area incubated with free radical scavenging detection. It was obvious that 13 compounds including myricetrin, myricetin-3-*O*-glycoside, myricetin-3-*O*-rutinoside, gallic acid, myricetin-3-*O*-neohesperidoside, quercitrin, isoquercitrin, isorhamnetin-3-*O*-glucoside, quercetin 3-*O*-rutinoside, kaempfero-3-*O*-*β*-*D*-glucoside, kaempferol-3-*O*-rhamnoside, isorhamnetin-3-*O*-rutinoside and quercetin 3-*O*-glucoside-dirhamnosyl were the principal components scavenging radical about ethyl acetate fraction, and regarded as the potential anti-oxidant candidate.

The anti-oxidant activity depends on the structure, location and number of hydroxyl groups. As shown in Fig. 4, the scavenging activity of myricetin derivatives was much higher than of other compounds. The B-ring of myricetin had 3,4,5-trihydroxy group,

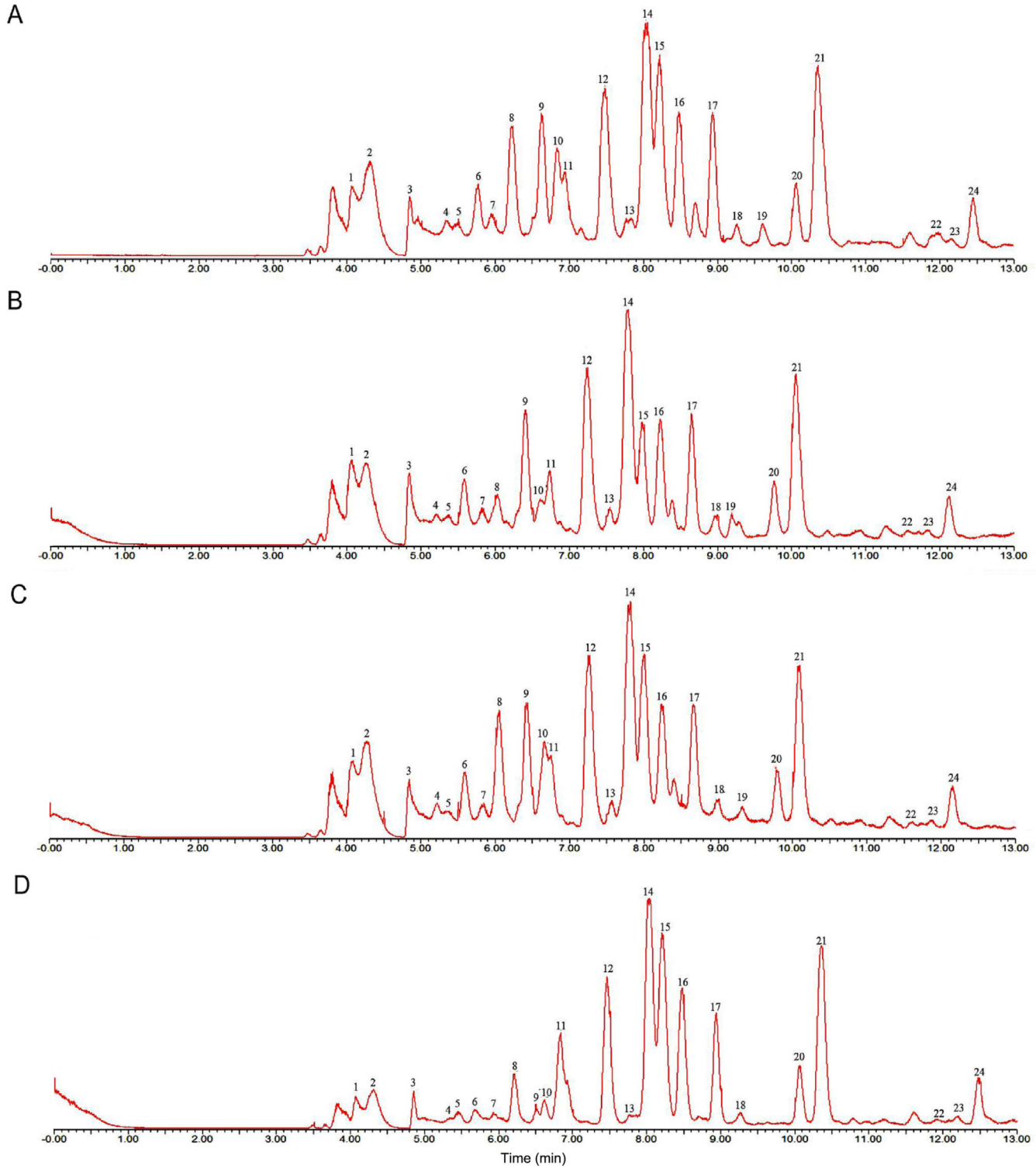


**Fig. 4.** Peak chromatograms of EtOAc obtained by UPLC-ESI-QTOF-MS in negative ion mode. Peaks are numbered according to Table 2. A: base peak chromatograms; B: chromatographic peaks detected by the UPLC-DPPH assays; C: chromatographic peaks detected by the UPLC-ABTS assays; D: chromatographic peaks detected by the UPLC-OH assays.

**Table 3**
Free radical scavenging activities of flowers of *X. sorbifolia*.

| Peaks | Compounds | Scavenging DPPH | | | Scavenging ABTS$^+$ | | | Scavenging OH | | | Average RP (%) |
|---|---|---|---|---|---|---|---|---|---|---|---|
| | | $A_0$ | $A_1$ | RP (%) | $A_0$ | $A_1$ | RP (%) | $A_0$ | $A_1$ | RP (%) | |
| 1 | Quercetin 3-*O*-glucoside-dirhamnosyl | 14 072.11 | 13 545.31 | 3.74 | 14 072.11 | 13 838.71 | 1.66 | 5 780.83 | 1 549.83 | 73.19 | 26.20 |
| 2 | Myricetin 3-*O*-neohesperidoside | 42 178.25 | 18 147.54 | 56.97 | 42 178.25 | 40 694.44 | 3.52 | 4 562.00 | 162.54 | 96.44 | 52.31 |
| 3 | Gallic acid | 2 246.17 | 1 825.32 | 18.74 | 2 246.17 | 1 928.58 | 14.14 | 2 268.19 | 331.71 | 85.38 | 39.42 |
| 4 | Isorhamnetin-3-*O*-dirhamnosyl | 7551.319 | 6 954.206 1 | 7.91 | 7 551.319 | 7 468.712 | 1.09 | 3 527.159 | 2 943.422 | 16.55 | 8.52 |
| 5 | Kaempferol-3-*O*-deoxyhexose-hexose | 7 049.411 | 593.089 4 | 10.23 | 7 049.411 | 6 841.737 | 2.95 | 1 916.816 | 1750.763 | 8.66 | 7.28 |
| 6 | Quercetin-3-*O*-dirhamnosyl-glucoside | 27 879.14 | 26 538.15 | 4.81 | 27 879.14 | 24 060.84 | 13.70 | 24 030.65 | 18 906.64 | 0.21 | 6.24 |
| 7 | Kaempferol-3-*O*-rhamnoside | 9 826.73 | 8 966.62 | 8.75 | 9 826.73 | 9 326.70 | 5.09 | 5 522.83 | 5 495.34 | 0.50 | 4.78 |
| 8 | Myricetin-3-*O*-rutinoside | 102 501.46 | 25 034.03 | 75.58 | 102 501.46 | 98 528.41 | 3.88 | 91 057.46 | 6 551.29 | 92.81 | 57.42 |
| 9 | Kaempferol-3-*O*-rutinoside-7-*O*-rhamnoside | 82 750.09 | 82 494.22 | 0.31 | 82 750.09 | 76 459.40 | 7.60 | 73 194.88 | 66 123.34 | 9.66 | 5.86 |
| 10 | Myricetin 3-*O*-glucoside | 66 004.62 | 16 275.23 | 75.34 | 66 004.62 | 62 350.13 | 5.54 | 53 851.21 | 4 264.61 | 92.08 | 57.65 |
| 11 | Quercetin 7-*O*-rutinoside | 45 746.40 | 44 621.21 | 2.46 | 45 746.40 | 39 151.00 | 14.42 | 37 672.01 | 25 242.39 | 32.99 | 16.62 |
| 12 | Quercetin 3-*O*-rutinoside | 173 060.08 | 147 257.72 | 14.91 | 173 060.08 | 15 0157.63 | 13.23 | 139 960.70 | 105 589.00 | 24.56 | 17.57 |
| 13 | Quercetin-7-*O*-dirhamnosyl-diglucoside | 4 350.33 | 3 953.12 | 9.13 | 4 350.33 | 4 190.67 | 3.67 | 2 162.85 | 1 836.27 | 15.10 | 9.30 |
| 14 | Kaempferol 3-*O*-neohesperidoside | 222 935.41 | 221 904.41 | 4.98 | 222 935.41 | 211 377.61 | 5.18 | 233 637.12 | 188 671.27 | 19.25 | 6.48 |
| 15 | Myricitrin | 147 615.30 | 9 268.78 | 93.72 | 147 615.30 | 140 162.91 | 5.05 | 118 050.75 | 29 484.26 | 75.02 | 57.93 |
| 16 | Isoquercitrin | 92 534.56 | 912 22.87 | 1.42 | 92 534.56 | 80 845.76 | 12.63 | 69 972.34 | 36 272.76 | 48.16 | 20.74 |
| 17 | Kaempferol-3-*O*-rutinoside | 103 296.36 | 99 986.69 | 3.20 | 103 296.36 | 92 868.72 | 10.09 | 68 220.59 | 61 336.76 | 10.09 | 7.80 |
| 18 | Isorhamnetin 3-*O*-rutinoside | 10 705.55 | 9 355.43 | 12.61 | 10 705.55 | 8 958.56 | 16.32 | 4 642.64 | 3 967.88 | 14.53 | 14.49 |
| 19 | Kaempferol-7-*O*-hexosyl(1–2) deoxyhexoside | 5 092.51 | 4 894.83 | 3.88 | 5 092.51 | 4 960.83 | 2.59 | 1 480.78 | 1 305.64 | 11.83 | 6.10 |
| 20 | Kaempferol 3-*O*-glucoside | 49 268.91 | 46 428.95 | 5.76 | 49 268.91 | 44 299.45 | 10.09 | 16 006.46 | 10 812.72 | 32.45 | 16.10 |
| 21 | Quercitrin | 132 933.52 | 105 172.28 | 20.88 | 132 933.52 | 123 784.77 | 6.88 | 61 740.91 | 35 757.41 | 42.08 | 23.28 |
| 22 | Chrysoeriol 7-*O*-glucoside | 1 771.31 | 1 482.07 | 16.33 | 1 771.31 | 1 663.78 | 6.07 | 833.34 | 799.53 | 4.06 | 8.82 |
| 23 | Isorhamnetin-3-*O*-glucoside | 3 678.74 | 3003.84 | 18.35 | 3 678.74 | 2 818.10 | 23.40 | 1605.45 | 1 324.71 | 17.49 | 19.74 |
| 24 | Kaempferol 7-*O*-rhamnoside | 36 926.65 | 32 396.48 | 12.27 | 36 926.65 | 30 638.84 | 17.03 | 20 101.01 | 17 082.71 | 15.02 | 14.77 |

the structure of which played an extremely important role in anti-oxidant activity. However, quercetin, kaempferol and isorhamnetin showed slightly lower activity than myricetin due to different hydroxyl groups (Cai, Mei, Jie, Luo, & Corke, 2006). Isorhamnetin derivatives exhibited higher activity than kaempferol derivatives, as it had 3′-methoxy in its B-ring. As the electron-donating groups, 3′-methoxy led to high anti-oxidant activity of isorhamnetin derivatives (Seyoum, Asres, & El-Fiky, 2006). Gallic acid exhibited higher activity, because its molecular structure was conjugated to the electron-donor group at the 4-location of the aromatic ring. However, the anti-oxidant activity did not always behave as described above. Rutin showed the same number and position of hydroxyl groups as quercetin, but it had lower anti-oxidant activity. This may be due to the fact that the molecular volume of rutin was larger than that of quercetin, which obstructed its clearance in space and reduced its anti-oxidant properties. The results revealed that the radical scavenging activities of the tested flavonoids were associated with the number and position of phenolic hydroxyl groups in the molecules.

### *3.4. Anti-hyperglycemic activity of ethyl acetate fraction in flowers of X. Sorbifolia*

#### *3.4.1. Ethyl acetate fraction in flowers of X. Sorbifolia ameliorated glucose tolerance in diabetic mice*

Free radicals were considered to be the contributing factors of diabetes which started early in the onset of diabetes and increased gradually. Meanwhile, excessive oxygen free radicals could also accelerate lipid aggregation, oxidize low-density lipoprotein to ox-LDL, stimulate endothelial cells to secrete a variety of inflammatory factors, which was advantageous to favor the formation of advanced glycation end products, leading to hepatocyte inflammation, injury, and cell death associated disorders, resulting in serious diabetic complications and liver disease. Thus, we assessed the impact of flowers of *X. sorbifolia* on diabetes mellitus in rats.

Diabetic mice induced by high-fat diet combined with a low dose of streptozocin and shared characteristics with human type II diabetes, which were widely used as an animal model to evaluate the metabolic disease. Glucose tolerance was an important indicator of type II diabetes. Compared with the control group (7.30 ± 0. 94 mmol/L), the OGTT levels of model group were increased significantly (24.60 ± 1.98 mmol/L). The mice in the model group had damaged glucose tolerance, and remained high blood glucose level after the gavage of glucose. Treatment with low (14.00 ± 2.22 mm ol/L), middle (19.80 ± 2.59 mmol/L), high (18.20 ± 2.96 mmol/L) EtOAc layers or metformin (14.60 ± 0.55 mmol/L) for 15 d significantly ameliorated damaged glucose tolerance. This result indicated that EtOAc layer obviously improved glucose tolerance in diabetic mice induced by streptozocin and high-fat diet (Fig. 5).

#### *3.4.2. Ethyl acetate fraction in flowers of X. Sorbifolia prevented the increased blood glucose*

Hyperglycemia is the main consequence of diabetes, which results from a deficiency in insulin secretion or degradation of produced insulin. After the streptozocin induction, model mice were developed hyperglycemia compared with normal mice. Nevertheless, the low (18.28 ± 0.12 mmol/L), middle (17.48 ± 0.17 mmol/L), high (17.28 ± 0.08 mmol/L) EtOAc groups or metformin (8.08 ± 0.04 mmol/L) treatment (over 15 days) had significantly hypoglycemic activities. In animal models of streptozocin-induced diabetes, blood glucose was the most intuitive indicators for detecting whether diabetes was improving. Our results showed that EtOAc layer reduced the blood glucose significantly.

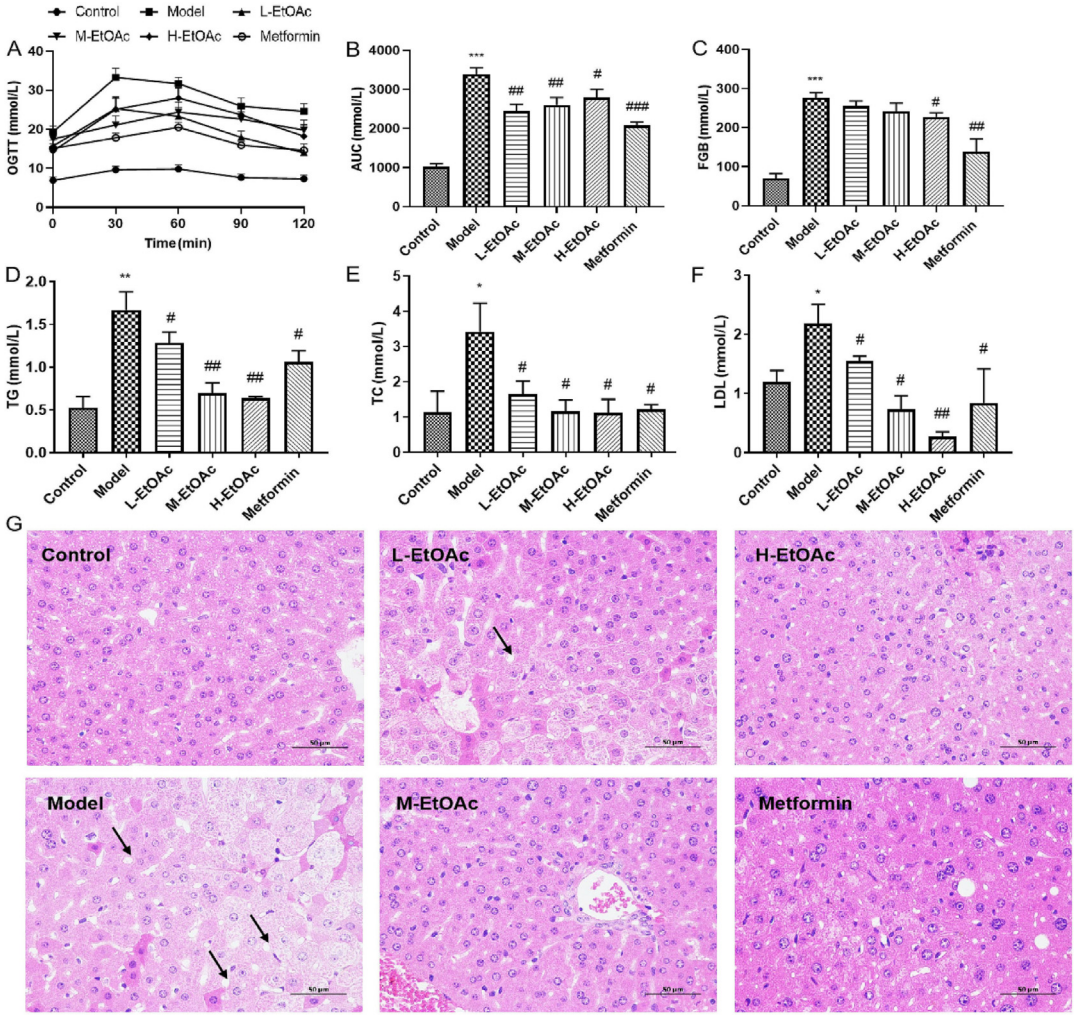


**Fig. 5.** Therapeutic effects of EtOAc on diabetic mice. A: Serum glucose data from OGTT; B: Area under the curve (AUC) of OGTT; C: Effect of EtOAc on fasting blood glucose (FGB); D: Effects of EtOAc on TG; E: Effects of EtOAc on TC; F: Effects of EtOAc on LDL-C; G: Histological examination of liver tissue (original magnification × 400, scale bar = 50 μm). Control, saline-treated group received a basal diet; Model, saline-treated group received a high-suger and high-fat diet and induced by STZ; L-EtOAc, L-EtOAc-treated group received a high-suger and high-fat diet and induced by STZ; M−EtOAc, M−EtOAc−treated group received a high-suger and high-fat diet and induced by STZ; H-EtOAcl, H-EtOAc-treated group received a high-suger and high-fat diet and induced by STZ; Metformin, Metformin-treated group received a high-suger and high-fat diet and induced by STZ. Statistical significance: $^{*}P < 0.05$, $^{**}P < 0.01$, $^{***}P < 0.001$ *vs* control group; $^{\#}P < 0.05$, $^{\#\#}P < 0.01$, $^{\#\#\#}P < 0.001$ *vs* model group.

### *3.4.3. Ethyl acetate fraction in flowers of X. Sorbifolia improved effects of lipid levels*

The serum levels of TC, TG and LDL-C in the diabetic model group increased significantly during the study compared with the levels in the normal control group ($P < 0.05$). EtOAc layer treatment over 15 d was observed to reduce TG, TC and LDL levels versus those observed in the model control group ($P < 0.05$). Therefore, these results suggested that it regulated lipid metabolism diabetic mice.

### *3.4.4. Ethyl acetate fraction in flowers of X. Sorbifolia relieved liver histology changes*

Histopathological analysis showed no significant histological changes in the liver of mice in the control group, while liver cells in the model group showed fatty changes, cell swelling, increased lipid droplets with lymphocyte infiltration and microvascular steatosis. Hepatocytes in the EtOAc layer 30 mg/kg group showed considerable histological recovery. EtOAc treated with 60 and 90 mg/kg significantly reduced and lost degenerative liver cells. The result showed that supplementation of flowers of *X. sorbifolia* was able to reduce OGTT, FGB, TG, TC, LDL-C to the level that of normal rats, and it reduced and lost degenerative liver cells clearly demonstrating the anti-oxidative potential of it.

### *3.4.5. Molecular docking results*

NADPH oxidase is an important endogenous pro-oxidant enzyme, the sole function of which is the generation of ROS, mainly superoxide. Though ROS acts as an important messenger in cellular signaling at normal concentration, overproduction of ROS and ele-

**Table 4**
Analysis results of main phenolic molecules and acarbose dockings into NADPH oxidase.

| Digestive enzymes | Main phenolics | T-score |
|---|---|---|
| NADPH oxidase | Quercetin 3-*O*-rutinoside | 7.232 |
| | Kaempferol-3-*O*-rhamnoside | 5.578 8 |
| | Isorhamnetin-3-*O*-glucoside | 5.033 3 |
| | Isoquercitrin | 4.888 2 |
| | Myricetrin | 3.916 7 |
| | Quercitrin | 3.551 8 |
| | Myricetin-3-*O*-rutinoside | 2.953 8 |
| | Myricetin-3-*O*-glycoside | 2.288 4 |
| | Isorhamnetin-3-*O*-rutinoside | 2.052 4 |
| | Myricetin-3-*O*-neohesperidoside | 1.230 4 |

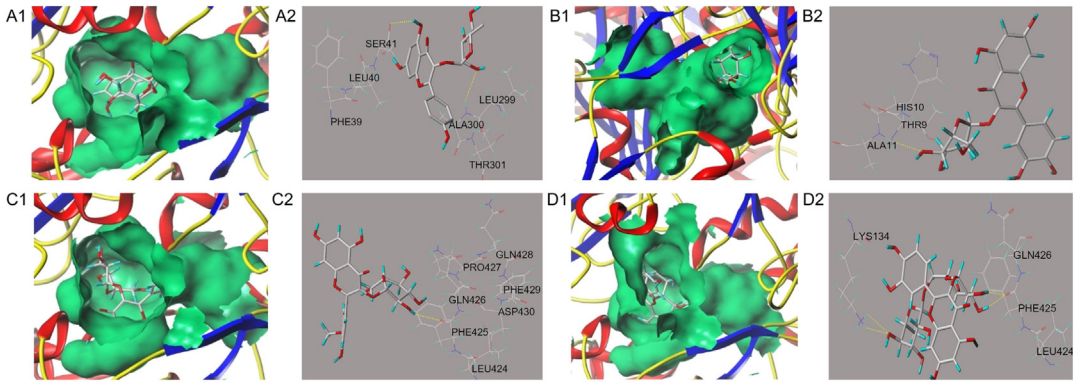


**Fig. 6.** Molecular docking of main four compounds with NADPH oxidase. The 3D docking structures of four main phenolic compounds were inserted into hydrophobic cavity of NADPH oxidase (green): kaempferol-3-*O*-rhamnoside (A1); isoquercitrin (B1); isorhamnetin-3-*O*-glucoside (C1); quercetin 3-*O*-rutinoside (D1). Conformation of active molecules interactions with amino acid residues in active site of NADPH oxidase: kaempferol-3-*O*-rhamnoside (A2); isoquercitrin (B2); isorhamnetin-3-*O*-glucoside (C2); quercetin 3-*O*-rutinoside (D2) with residues in active sites of the NADPH oxidase, respectively. Dashed line stands for hydrogen bonds.

vated oxidative stress lead to alterations in endogenous non-enzymatic and enzymatic defence systems. Therefore, molecular docking analysis was further done to analyze the NADPH oxidase inhibitory mechanisms of the main 13 compounds which were screened by off-line UPLC-QTOF-MS/MS-free radical scavenging. Table 4 showed the molecular docking results with regard to interactions between NADPH oxidase and ten main molecules binding which three compounds were rejected because of the negative docking values with the oxidase. From Table. 4, the molecular docking total-scores values of four molecules were all $\geq 4$, which indicated credible docking results. Fig. 6 clearly revealed that the structures of four compounds significantly affect their inhibitory effects on NADPH oxidase. Kaempferol-3-*O*-rhamnoside interacted with the active sites of NADPH oxidase and formed two H-bonds (yellow dotted line) with four amino acid residues (Ser 41, Ala 300, Leu 299, Thr 301). Isoquercitrin formed one H-bonds with three amino acid residues, namely Ala 11, Thr 9, His 10. Isorhamnetin-3-*O*-glucoside formed one H-bonds with seven amino acid residues, namely Gln 426, Gln 428, Pro 427, Phe 425, Phe 429, Asp 430, Leu 424. It was found that quercetin 3-*O*-rutinoside formed four H-bonds with four amino acid residues, namely Lys 134, Gln 426, Phe 425, Leu 424.

The results demonstrated that the inhibition of NADPH oxidase by kaempferol-3-*O*-rhamnoside, isoquercitrin, isorhamnetin-3-*O*-glucoside, quercetin 3-*O*-rutinoside could be correlated with the results presented by Araújo et al., which showed that the main compounds exhibited anti-oxidant activity, inhibited subunit $p47^{phox}$ phosphorylation of NADPH oxidase, decreased NADPH oxidase activity and inhibited the neutrophil ROS production (Araújo et al, 2017; Li et al, 2014).

## 4. Conclusion

The phytochemical and biological investigation of flowers of *X. sorbifolia* revealed that this plant was a rich source of flavonoids and phenolic acids with significant anti-oxidant activities and showed the activity of suppressing hyperglycemia and NADPH oxidase related to type 2 diabetes. Overall, flowers of *X. sorbifolia* with a good potential to be further explored as a new source of tea.

## CRediT authorship contribution statement

**Xiajing Xu:** Formal analysis, Writing-original draft, Data visualization. **Yongli Guo:** Formal analysis. **Menglin Chen:** Formal analysis. **Ning Li:** Experimental supervision. **Yi Sun:** Experimental supervision. **Shumeng Ren:** Writing-editing. **Jiao Xiao:** Writing-editing. **Dongmei Wang:** Writing-editing. **Xiaoqiu Liu:** Writing-review & editing. **Yingni Pan:** Writing-review & editing.

## Declaration of Competing Interest

The authors declare that they have no known competing financial interests or personal relationships that could have appeared to influence the work reported in this paper.

## Acknowledgements

The financial support of this study was from the Fourth National Investigation of Chinese materia medica resources in Liaoning Province (LN2018017, LN2019019); Career Development Support Plan for Young and Middle-aged Teachers in Shenyang Pharmaceutical University (No. ZQN2021014); and Key Laboratory of Marine Biogenetic Resources, Ministry of Natural Resources (No. HY202105).

## References

Araújo, G. R., Rabelo, A. C., Meira, J. S., Rossoni-Júnior, J. V., Castro-Borges, W., Guerra-Sá, R., ... Costal, D. C. (2017). *Baccharis trimera* inhibits reactive oxygen species production through PKC and down-regulation $p47^{phox}$ phosphorylation of NADPH oxidase in SK Hep-1 cells. *Experimental Biology and Medicine, 242*(3), 333.

Bi, Q., Cai, L., Ma, X., Yang, H., & Guan, W. (2011). Review on genetics and industrialization of *Xanthoceras sorbifolia* Bge., an indigenous energy species in China. *Chinese Wild Plant Resources, 30*, 37–41.

Braunberger, C., Zehl, M., Conrad, J., Fischer, S., Adhami, H. R., Beifuss, U., & Krenn, L. (2013). LC-NMR, NMR, and LC-MS identification and LC-DAD quantification of flavonoids and ellagic acid derivatives in *Drosera peltata*. *Journal of Chromatography B, 932*, 111–116.

Cai, Y. Z., Mei, S., Jie, X., Luo, Q., & Corke, H. (2006). Structure-radical scavenging activity relationships of phenolic compounds from traditional Chinese medicinal plants. *Life Sciences, 78*, 2872–2888.

Cao, J., Xia, X., Chen, X., Xiao, J., & Wang, Q. (2013). Characterization of flavonoids from *Dryopteris erythrosora* and evaluation of their anti-oxidant, anti-cancer and acetylcholinesterase inhibition activities. *Food and Chemical Toxicology, 51*, 242–250.

Etsassala, N. G. E. R., Badmus, J. A., Marnewick, J. L., Egieyeh, S., Iwuoha, E. I., Nchu, F., & Hussein, A. A. (2020). Alpha-glucosidase and alpha-amylase inhibitory activities, molecular docking, and anti-oxidant capacities of *Plectranthus ecklonii* constituents. *Anti-oxidants, 9*(11), 1149.

Gao, M. R., Chen, L., He, Q., Sun, Q., & Zeng, W. C. (2018). Influence of different methods and standards on the determination of total phenol contents. *Chinese Journal of Analysis Laboratory, 37*, 1053–1056.

Godoy, P., Hewitt, N. J., Albrecht, U., Andersen, M. E., Ansari, N., Bhattacharya, S., ... Glanemann, M. a. (2013). Recent advances in 2D and 3D *in vitro* systems using primary hepatocytes, alternative hepatocyte sources and non-parenchymal liver cells and their use in investigating mechanisms of hepatotoxicity, cell signaling and ADME. *Archives of Toxicology, 87*, 1315–1530.

Guo, L., Tan, D. C., Bao, R. J., Sun, Q., Xiao, K. M., Xu, Y., ... Hua, Y. (2020). Purification and anti-oxidant activities of polyphenols from *Boletus edulis* Bull.: Fr. *Journal of Food Measurement and Characterization, 14*, 649–657.

Hui, C., Ouyang, K., Yan, J., Yang, Z., Hu, W., Lei, X., ... Wang, W. (2017). Constituent analysis of the ethanol extracts of *Chimonanthus nitens* Oliv. leaves and their inhibitory effect on alpha-glucosidase activity. *International Journal of Biological Macromolecules, 98*, 829–836.

Jessica, P., Dorothée, G., Aurélie, C., Florence, B., Anthony, D., Cynthia, P., ... Philippe, R. (2017). Diabetes-induced hepatic oxidative stress: A new pathogenic role for glycated albumin. *Free Radical Biology and Medicine, 102*, 133–148.

Jiang, M., Zhang, W., Zhang, T., Liang, G., Hu, B., Han, P., & Gong, W. (2020). Assessing transfer of pesticide residues from chrysanthemum flowers into tea solution and associated health risks. *Ecotoxicology and Environmental Safety, 187*, 109859.

Khallouki, F., Ricarte, I., Breuer, A., & Owen, R. W. (2018). Characterization of phenolic compounds in mature Moroccan Medjool date palm fruits (*Phoenix dactylifera*) by HPLC-DAD-ESI-MS. *Journal of Food Composition and Analysis, 70*, 63–71.

Li, Q., Qiu, Y., Mao, M., Lv, J., Zhang, L., Li, S., ... Zheng, X. (2014). Anti-oxidant mechanism of rutin on hypoxia-induced pulmonary arterial cell proliferation. *Molecules, 19*, 19036–19049.

Li, N., Wang, Y., Li, X., Zhang, H., Zhou, D., Wang, W., ... Meng, D. (2016). Bioactive phenols as potential neuroinflammation inhibitors from the leaves of *Xanthoceras sorbifolia* Bunge. *Bioorganic & Medicinal Chemistry Letters, 26*, 5018–5023.

Li, W., Lu, Q., Li, X., Liu, H., Sun, L., Lu, X., ... Liu, P. (2020). Anti-Alzheimer's disease activity of secondary metabolites from *Xanthoceras sorbifolia* Bunge. *Food & Function, 11*, 2067–2079.

Li, Y., Chen, D., Zhang, F., Lin, Y. P., Ma, Y. G., Zhao, S. L., ... Liu, J. (2020). Preventive effect of pressed degreased walnut meal extracts on T2DM rats by regulating glucolipid metabolism and modulating gut bacteria flora. *Journal of Functional Foods, 64*, 103694.

Ma, Y., Feng, Y., Diao, T., Zeng, W., & Zuo, Y. (2020). Experimental and theoretical study on anti-oxidant activity of the four anthocyanins. *Journal of Molecular Structure, 1204*, 127509.

Mazumdar, S., Marar, T., Devarajan, S., & Patki, J. (2021). Functional relevance of Gedunin as a bona fide ligand of NADPH oxidase 5 and ROS scavenger: An *in silico* and *in vitro* assessment in a hyperglycemic RBC model. *Biochemistry and Biophysics Reports, 25*, 100904.

Najafi, F., Kavoosi, G., Siahbalaei, R., & Kariminia, A. (2022). Anti-oxidative and anti-hyperglycemic properties of *Agastache foeniculum* essential oil and oily fraction in hyperglycemia-stimulated and lipopolysaccharide-stimulated macrophage cells: *In vitro* and *in silico* studies. *Journal of Ethnopharmacology, 284*, 114814.

Qi, G., Yang, A., Zheng, Z., Han, N., Zhang, F., & Shang, H. (2019). Study on anti-oxidant activity and anti-bacterial activity of the shell extracts of *Xanthoceras sorbifolia*. *Acta Chinese Medicine and Pharmacology, 47*, 58–60.

Seyoum, A., Asres, K., & El-Fiky, F. K. (2006). Structure-radical scavenging activity relationships of flavonoids. *Phytochemistry, 67*, 2058–2070.

Tkacz, K., Wojdylo, A., Turkiewicz, I. P., Ferreres, F., Moreno, D. A., & Nowicka, P. (2020). UPLC-PDA-Q/TOF-MS profiling of phenolic and carotenoid compounds and their influence on anti-cholinergic potential for AChE and BuChE inhibition and on-line anti-oxidant activity of selected *Hippophae rhamnoides* L. cultivars. *Food Chemistry, 309*, 125766.

Tounekti, T., Joubert, E., Hernandez, I., & Munne-Bosch, S. (2013). Improving the polyphenol content of tea. *Critical Reviews in Plant Sciences, 32*, 192–215.

Unuofin, J. O., & Lebelo, S. L. (2021). UHPLC-QToF-MS characterization of bioactive metabolites from *Quercus robur* L. grown in South Africa for anti-oxidant and anti-diabetic properties. *Arabian Journal of Chemistry, 14*, 102970.

Vieira, G. S., Marques, A. S. F., Machado, M. T. C., Silva, V. M., & Hubinger, M. D. (2017). Determination of anthocyanins and non-anthocyanin polyphenols by ultra performance liquid chromatography/ electrospray ionization mass spectrometry (UPLC/ESI-MS) in jussara (*Euterpe edulis*) extracts. *Journal of Food Science and Technology, 54*, 2135–2144.

Wang, C. X., Pu, B., Jiang, Y., & Fu, B. N. (2017). Extraction and anti-oxidant activity *in vitro* of flavonoids in cold pressed cake of *Zanthoxylum armatum* DC. *Prodr. Food & Machinery, 33*, 137–143.

Wang, D., Su, D., Li, X. Z., Liu, D., Xi, R. G., Gao, H. Y., & Wang, X. B. (2016). Barrigenol triterpenes from the husks of *Xanthoceras sorbifolia* Bunge and their anti-tumor activities. *Rsc Advances, 6*(33), 27434–27446.

Wang, X., Zhao, X., Gu, L., Zhang, Y., Bi, K., & Chen, X. (2014). Discrimination of aqueous and vinegary extracts of Shixiao San using metabolomics coupled with multivariate data analysis and evaluation of anti-hyperlipidemic effect. *Asian Journal of Pharmaceutical Sciences, 9*, 17–26.

Wang, Y., Jiang, S., Meng, D. L., & Li, N. (2011). Advances in study on chemical and biological activity of *Xanthoceras sorbifolia*. *Drugs and Clinic, 26*, 269–273.

Wu, L. F., Liu, Y. F., Qin, Y., Wang, L., & Wu, Z. Q. (2019). HPLC-ESI-qTOF-MS/MS characterization, anti-oxidant activities and inhibitory ability of digestive enzymes with molecular docking analysis of various parts of raspberry (*Rubus ideaus* L.). *Anti-oxidants, 8*, 274.

Wu, Y., Jiang, X., Zhang, S., Dai, X., Liu, Y., Tan, H., ... Xia, T. (2016). Quantification of flavonol glycosides in *Camellia sinensis* by MRM mode of UPLC-QQQ-MS/MS. *Journal of Chromatography B, 1017–1018*, 10–17.

Yang, Z., Li, Z., & Li, Z. (2018). DPPH-HPLC-MS assisted rapid identification of endothelial protective substances from Xiao-Ke-An. *Journal of Ethnopharmacology, 211*, 188–196.

Yao, Z. Y., Qi, J. H., & Yin, L. M. (2013). Biodiesel production from *Xanthoceras sorbifolia* in China: Opportunities and challenges. *Renewable & Sustainable Energy Reviews, 24*, 57–65.

Zhang, G., Luo, S., Huan, G. J., Cai, X., & Zhang, Y. (2018). Determination of total flavonoids in mulberry leaf extract by aluminium trichloride colorimetric method. *Farm Products Processing, 7*, 52–54.

Zhao, L., Li, X., Ye, Z. Q., Zhang, F., Han, J. J., Yang, T., ... Zhang, Y. (2018). Nutshell extracts of *Xanthoceras sorbifolia*: A new potential source of bioactive phenolic compounds as a natural anti-oxidant and immunomodulator. *Journal of Agricultural and Food Chemistry, 66*, 3783–3792.

Zhao, Y., Wang, Y., Jiang, Z. T., & Li, R. (2017). Screening and evaluation of active compounds in polyphenol mixtures by HPLC coupled with chemical methodology and its application. *Food Chemistry, 227*, 187–193.

Zheng, J., Tian, W., Yang, C., Shi, W., Cao, P., Long, J., ... Sun, P. (2019). Identification of flavonoids in plumula nelumbinis and evaluation of their anti-oxidant properties from different habitats. *Industrial Crops and Products, 127*, 36–45.